

## DIGITAL PHOTOGRAMMETRY, GPR AND FINITE ELEMENTS IN HERITAGE DOCUMENTATION: GEOMETRY AND STRUCTURAL DAMAGES

P. Arias \*, J. Armesto, H. Lorenzo, C. Ordóñez

Dep. Natural Resources Engineering and Environmental Engineering, University of Vigo, Campus Universitario As Lagoas – Marcosende s/n 36200 Vigo Spain – (parias, julia, hlorenzo, cgalan)@uvigo.es

**KEY WORDS:** Close Range Digital Photogrammetry, GPR, Structural analysis, Structural Damages Surveying, Cultural Heritage, Documentation Techniques.

### ABSTRACT:

This paper shows a multidisciplinary approach to heritage documentation involving Close Range Photogrammetry and Ground Penetrating Radar techniques, as well as the development of finite elements based structural models. The geometric shape, the building material homogeneity and the current damages and its causes are obtained. The usefulness of Close Range Photogrammetry in the accurate 3D modelling and cracks detection and mapping is analyzed. Further, a non destructive test through GPR is employed for the interior material homogeneity analysis and zones description. For both techniques, the methodology followed for data collection and data processing aimed at minimisation of time consuming and optimisation of results is described in detail. Resulting information related to the whole bridge geometry is taken as basis to develop different numeric models applying the finite elements method (FEM). This analysis involves different load hypothesis in order to obtain a stress distribution compatible with the detected damages which allows identifying likely causes of them.

### 1. INTRODUCTION

The interest of the study of traditional architectonic heritage lays in the fact that it is witnesses of the ways of life and the history of the modern societies, and characterizes the landscape of a region, as it is one of its main elements. Nowadays it is assumed that the architectonic cultural heritage is a fragile and irreplaceable resource. Nevertheless Spanish heritage protection policies have revealed to be frequently inefficient and in some monuments the course of time has developed into a noticeable deterioration of materials and degradation of the whole or parts of the structure. The planning of preservation and restoration interventions in architectural heritage monuments might be based on an accurate updated documentation of all what concerns the geometric shape, the architectural characteristics, the characteristics of materials and the structural analysis in order to locate highly stressed areas where fractures might emerge and identify likely causes of current cracks (Genovese, 2005). This all information should be taken as a decision tool to plan strengthening interventions or restoration actions.

Unfortunately, many technicians actually involved in heritage conservation still work on the documentation of monuments in a rather traditional way. However, in the last years some interesting approaches have been developed involving the application of new technologies to heritage documentation. Some examples related to heritage monuments 3D modelling through Digital Photogrammetry can be found in Alby et al. (2003), Toz and Duran (2004), Guidi et al. (2004), Arias et al. (2005); it might be pointed out that the application of this technology to bridges modelling have just recently started to be accomplished (see Jáuregui, 2005) probably due to the structural complexity of this kind of constructions. Ground Penetrating Radar (GPR) has been applied to the heritage documentation field by Flint et al (1999), Maierhofer and Leipold (2001), Ranalli et al (2004); specifically in masonry bridges in Colla et al. (1997) and Clark and Forde (2003). Finally interesting contributions to the structural analysis of bridges through finite elements can be found in Pegon et al. (2001), Lourenço (2002), Milani et al. (2006).

These all approaches have focused in specific fields of the monuments documentation: 3D modelling, analysis of building material, structural analysis or others. In the last years several conservationist's and restoration's have asserted the importance of adopting documentation protocols including advanced non contact surveying techniques and rigorous scientific analysis methods to document the cultural heritage properties and current state of decay (Genovese, 2005).

In this paper a multidisciplinary approach to heritage documentation is presented. Close Range Digital Photogrammetry and GPR techniques are used in the geometric survey, building material homogeneity analysis; they are also employed in cracks detection and mapping, since cracks are the external appearance of severe structural problems. Resulting information is used to properly define a finite elements based structural model (FEM), which is used to model the structural behaviour of the bridge in several load hypotheses. Results are compared to the cracks mapping. This comparison allows inferring the likely causes of the current state of decay in the bridge. This methodology has been tested in the Fillaboa Bridge, a masonry monument which date back from the roman period and is placed over the Tea River, in the *Salvaterra de Miño* Council, Northwest of Spain.

### 2. INSTRUMENTATION

- Digital calibrated non-metric camera, Canon EOS 10D, 6,291,456 pixels CCD resolution. The calibration process was performed without zoom lens for the minimum diaphragm (maximum field of view). Calibration parameters are shown in table 1.
- Circular paper targets with cross points.
- Monoscopic digital photogrammetric station. This system is based on the software package Photomodeler Pro 5.0. It is used for the orientation and restitution processes. The results are obtained in a graphic format (DXF; 3D Studio,

\* Corresponding author: Tel.: +34 986 813645; fax: +34 986813644.  
E-mail address: [parias@uvigo.es](mailto:parias@uvigo.es) (P. Arias).

- RAW, VRML 1.0 and 2.0, Direct 3D, Wavefront and Iges formats are also available).
- Total station: Leica TPS 1100.
- Ground penetrating radar GPR-RAMAC with 250, 500, 800 MHz biestatic antennae.
- Rambshell software for FEM analysis.

|                        |                   |
|------------------------|-------------------|
| Focal length (mm)      | 20,2157           |
| Principal point (mm)   | 11,1601; 7,5245   |
| Radial distortion (mm) | A1: 0,000226      |
|                        | A2: -0,0000004906 |

Table 1. Calibration parameters of the Canon EOS 10D camera.

### 3. THE BRIDGE DOCUMENTATION

The documentation of the Fillaboa Bridge (see figure 1) has been sequenced in three steps, which are explained in detail in this section. The photogrammetric process is aimed at the geometric survey through the obtaining of the corresponding 3D accurate wire-frame model of the bridge and at the crack detection and mapping. The second step consisted on a non destructive test through GPR aimed at the analysis of the homogeneity of the interior material in the bridge and the detection of internal holes or cracks. Finally, a finite element model is constructed on the basis of the photogrammetric 3D model and the information derived from the material homogeneity analysis, considering different load hypothesis. The crack mapping derived from the first step is taken as reference for the hypothesis confirmation or rejection.



Figure 1. A roman masonry bridge (Fillaboa Bridge), in the *Salvaterra de Miño* Council, Northwest of Spain.

#### 3.1. The Photogrammetric process

Close Range digital Photogrammetry is a non-contact digitizing technique to measure size and shape of an object obtained from some photographs instead by direct measure. The last goal of the photogrammetric process is obtaining a 3D wire-frame model accurately representing the bridge geometry and a 3D photorealistic model properly containing the textures of the bridge. The standard procedure to survey an object through Digital Photogrammetry is described in Benko et al. (2001). The main steps are: data collection; data processing; restitution and 3D modelling. In this study a digital monoscopic system has been employed because it is considered more feasible in heritage documentation applications in terms of cost-efficiency balance than stereoscopic photogrammetry, single image processing procedures, or even laser scanner based surveys. This technique relies on the digital reconstruction of the object from several images taken from different and convergent perspectives to ensure a suitable geometry of intersecting rays.

A digital calibrated non-metric camera, Canon EOS 10D, 6,291,456 pixels CCD resolution, was used. Prior to the data collection performance, circular paper-targets were placed all along the longitudinal axis in both North and South bridge tympanums and also around arch's basis. Shots were taken from the upper path of the bridge and from both sides of the river, either upstream, downstream or below the arches, trying to satisfy overlapping and convergence conditions (see Cooper and Robson, 2001). The ground coordinates of the cross points within the paper-targets were precisely measured through the topographic total station Leica TPS 1100.

The data processing was performed through a monoscopic photogrammetric station. Six common points were identified in each pair of convergent photographs for the relative orientation of them. The photogrammetric network levelling and scaling was performed identifying the circular targets in the photographs and assigning the measured coordinates to its middle cross point. Finally a convergent bundle adjustment was performed.

A manual mode for the restitution process was followed in order to achieve the maximum accuracy in the resulting 3D models. Boundary points in the exterior face of the bridge stones were restituted. Then the corresponding boundary line of each stone in the bridge is defined. As a result a 3D wire-frame model is obtained for the whole bridge. Then a Delaunay triangulation is performed to obtain a non continuous model where sets of triangles have been fitted to the stones surface; photo-realistic textures are applied to each surface in order to obtain a 3D photorealistic model.

#### 3.2. The GPR test

Ground penetrating radar is a remote sensing and geophysical method based on the emission of a very short electromagnetic pulse (1-20 ns) in the frequency band of 10 MHz - 2.5 GHz. By moving the antennae over the ground, an image of the shallow subsurface under the displacement line is obtained. These images, called radargrams, are XZ graphic representations of the reflections detected where X axis represents antennae displacement and Z axis represents the two-way travel time of the pulse emitted.

In the study case the data were collected using 250, 500 and 800 MHz bistatic antennae. Three parallel profiles were recorded with each antenna, moving the system along the bridge, obtaining nine 85 m long radargrams. Radargrams were acquired with a trace interval of 2 cm and time window of 250 ns, 125 ns and 70 ns respectively, taking into account their different depth penetration and vertical resolution. The profiles were filtered to enhance the internal reflections from the bridge and from the interface between ashlar arches and air; main filter applied were: Dewow (DC removal), Max Phase correction, Geometrical Divergence Compensation (gain), and Band Pass (butterworth: 50/450). The photogrammetric measurements were used to obtain variations on the elevation of the profiles along the bridge, what allows applying the Static Correction and eliminate this effect on the radargrams.

#### 3.3. Generating the finite element model

Given the complexity in the determination of the structural response of masonry structures with complex geometry, as the historical bridges use to be, the use of numerical methods of analysis such as the finite elements method is required. The finite elements based models aimed to analyze the behaviour of

the rubblework should be non-linear because the mortar has a strong non-linear behaviour that is transferred to the whole of the rubblework due to the appearance of micro and macro fissures (Milani et al., 2006). However, every non-linear analysis should start with a linear analysis in order to determine the type and scope of the non-linearity of the problem (Bathe, 1996). Likewise, even the imperfect linear analysis can give very valuable information about certain failure mechanisms that in most of the cases escape the experts' intuition, as will be demonstrated.

Once the 3D model is obtained, the numeric modelling is accomplished. The parameters related to the building material are established on the base of the GPR test results. In relation to the loading parameters, two different boundary conditions have been analyzed. First of all, the structure perfectly supported by the plane of foundation has been considered. Such link is related to the structure working under normal conditions. Secondly, it has been considered that one of the central piers suffers from a relative descend in the third part of its support downstream. Such relative descend has been taken into account using a linear elastic support with an elastic coefficient calculated under the basis of a ballast coefficient equal to  $6.0e7 \text{ N/m}^3$ . The actions on the structure that have been taken into account in the analysis are the self-weight ( $2.3e4 \text{ N/m}^3$ ), the filling weight ( $1.8e4 \text{ N/m}^3$ ) and the traffic overload ( $3.0e3 \text{ N/m}^2$ ).

The principal stress diagram has been chosen for the analysis of results as it is the most representative result of the bridge structural behaviour. The values of the mechanical properties of the material are shown in Table 2 (Pegon et al, 2001).

|                     |                              |       |
|---------------------|------------------------------|-------|
| Young module        | E [N/m <sup>2</sup> ]        | 5e10  |
| Poisson coefficient | $\nu$ [-]                    | 0.15  |
| Specific weight     | $\gamma$ [N/m <sup>3</sup> ] | 18000 |

Table 2: Mechanical properties of the material.

## 4. RESULTS AND DISCUSSION

### 4.1. The Photogrammetric results

In the data collection step several difficulties for keeping theoretical overlapping and convergence conditions arose from the narrowness of the bridge on one side and the impossibility of taking shots from mid river bed on the other side. The accessible locations were just the upper path and the river sides. The upper path was used for photographing the handrails, the own path and the cutwaters up and downstream; but given the small width of the path 114 were needed for recording it ensuring adequate overlapping between consecutive photographs; 12 shots were taken for the cutwaters. From the river sides, the bridge tympanums and the bottom of arches were photographed: 34 were taken upstream, 34 downstream, 12 below the arches. The convergence angles varied from  $50^\circ$  to  $100^\circ$  (for the middle arch). The whole of 130 control points were measured.

The precise restitution of points in a masonry structure has revealed to be a hard slow process due to the advanced erosion state of the stones edges and the absence of vertexes or references that could be easily recognised in two different photographs. The paper-targets and mainly the rock crystals in the bridge stones were used for this end. But given its small size and different aiming view in each photograph, highly detailed views of the stones were needed for its restitution, involving

time consume, as well as several reviewing steps for relocating those points whose high error values revealed a wrong position. A cloud of 41.393 points was finally obtained. In spite of these difficulties a 3D wire-frame model accurately representing the bridge geometry was obtained (see figure 2): high accuracy values corresponding to the photogrammetric model points have been achieved (see table 3).

|                          | Average | Maximum |
|--------------------------|---------|---------|
| X (mm)                   | 5,5     |         |
| Y (mm)                   | 5,9     |         |
| Z (mm)                   | 4,3     |         |
| RMS residual (pixel)     | 0,97    |         |
| Maximum Residual (pixel) |         | 3.94    |

Table 3. Points position error (95% confidence), RMS and Maximum Residual.

The 3D model allowed detecting longitudinal cracks in the bottom of the middle arch and in the next arch on its right; cracks in the cutwater between both arches were also detected (see figure 3).

On the basis of the 3D wire-frame model, the photo-realistic textured model was obtained. The digital photogrammetric recording provides qualitative information about the bridges stones arrangement. The whole bridge is made of granite ashlar with varying sizes and narrow mortar joints. They are arranged longitudinally in the tympanums, cutwaters and bottom of arches, vertically in the handrails and in a radial direction in the arches boundaries. Stones in the tympanums are quite smaller and more heterogeneous than the rest.

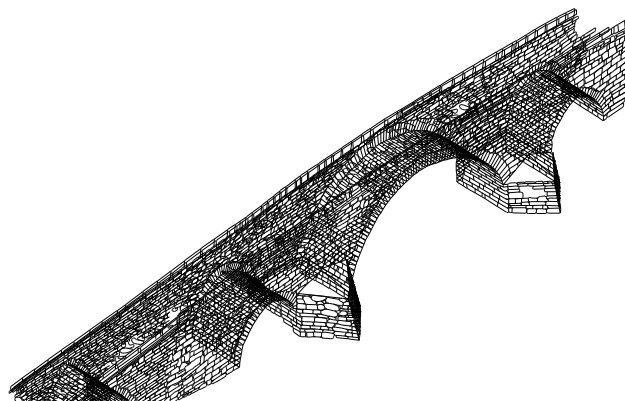


Figure 2. Fillaboa Bridge: 3D wire frame model.

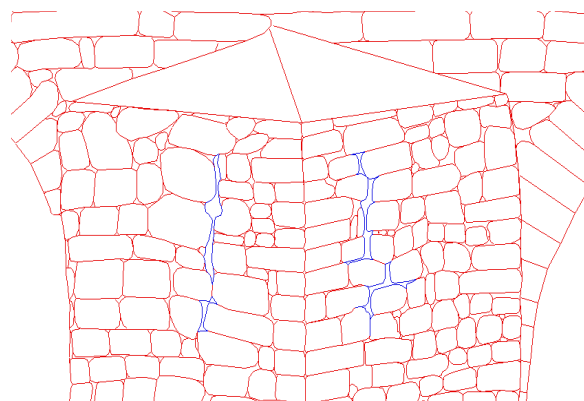


Figure 3. Cracks detection and mapping.

#### 4.2. The GPR test results

The signal of the higher frequency antennas (800 MHz) showed to be very attenuated in the two-way travel, and some of the arches are not recognizable in the radargrams obtained with such antennas, especially those which are deeper in relation to the bridge surface. On the contrary, the pulse of the 250 MHz antenna crossed the whole bridge. Resulting profiles showed relevant information about its internal structure, being possible to point out the reflections related to the foundations of the bridge (Figure 4). In the radargrams there are no evidences of very big internal cracks, neither reflections related to cavities, holes or similar. The resulting profiles showed that the backing (filling material) is quite homogeneous.

The averaged velocity of the radar pulse was estimated on 13 cm/ns for the backing and 16.5 cm/ns for the masonry, which fit with the expected values for these materials (Binda et al, 1998; Clark & Forde, 2003). These values for the velocities were calculated using the metric information given by the photogrametric survey, which allows an accurate known of the geometry of the arches and the distances between the surface of the bridge and the arches or the foundations.

#### 4.3. Structural analysis results

The bridge was discretized with a mesh of 3436 finite elements Reissner-Mindlin shell of six-node (see Figure 5). The bridge

walls were considered as homogeneous material with an isotropous linear elastic behaviour. It has been considered that the bridge filling does not have a resistant function. This consideration is justified by the historical documentation about the constructive techniques used in similar bridges. The results of the GPR analysis confirm this hypothesis.

The compression principal stress distribution, obtained by considering the structure perfectly supported on the plane of foundation and with no elastic supports, is presented in Figure 6. The structure arches working under normal conditions show a compression principal stress field parallel to the bridge axis. In the frontal walls, the compression principal stress field follow the geometry of the arches. Tensile principal stress field appears on the upper part of the pier, but the values are not significant (less than  $0.2\text{MN/m}^2$ ) compared to the compression principal stress values. (NBE FL-90)

The structure analyzed with a relative descend of the central pier presents, in the frontal walls and the lateral arches, a compression principal stress field quite similar to the obtained for the structure working under normal conditions (see Figure 7). The central arches present a compression principal stress field that slightly diverge from the axis of the bridge. This compression principal stress field point to the stiffest part of the pier support (upstream). Likewise, the central arches present a tensile principal stress field normal to the axis of the bridge (see Figure 8).

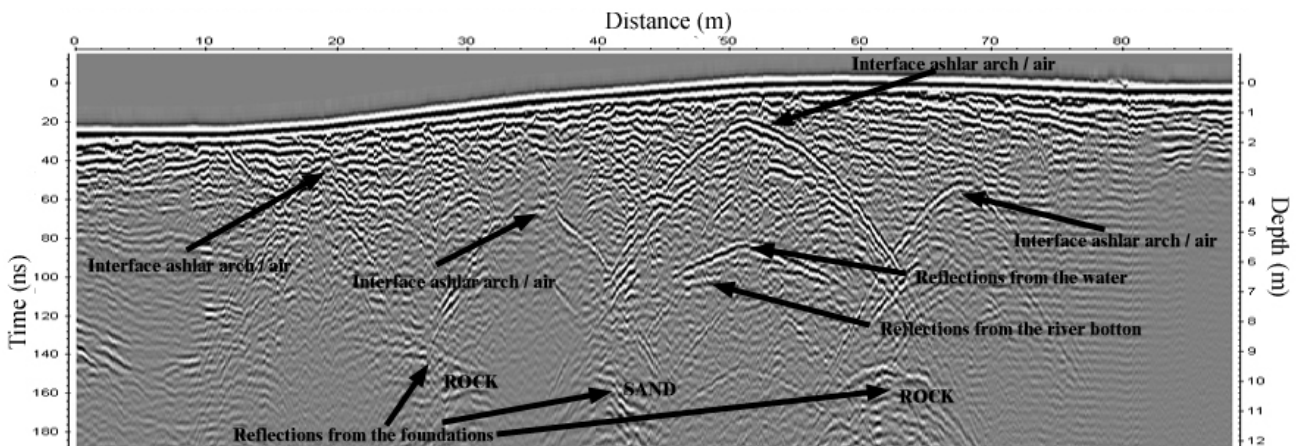


Figure 4. GPR test: 85 m long radargram obtained with the 250 MHz antenna (up) together with the interpretation of some reflections and diffractions detected in it.

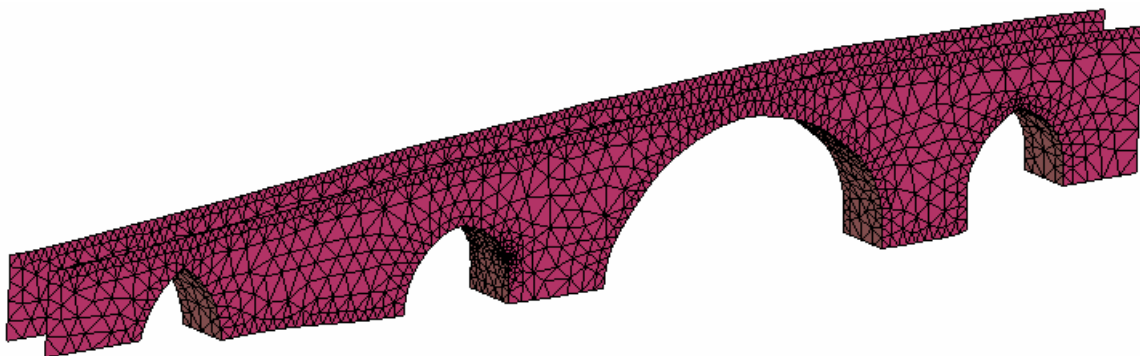


Figure 5: Mesh of finite elements used in the structure analysis.

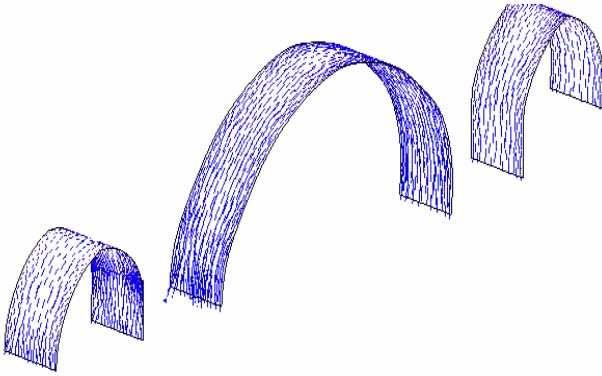


Figure 6. Compression principal stress diagram in the central arches.

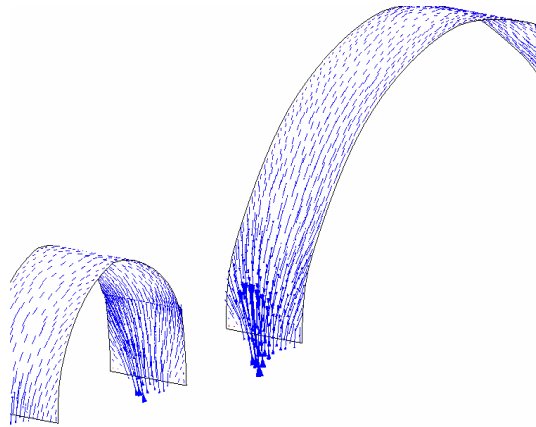


Figure 7. Compression principal stress diagram in the main arches.

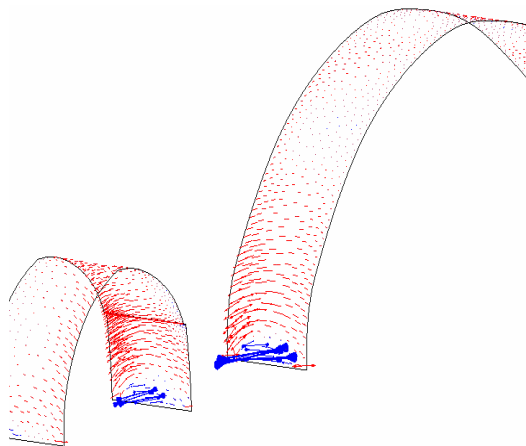


Figure 8. Tensile principal stress diagram in the central arches.

Comparing the results obtained from both of the established hypothesis and the photogrammetric documentation, it is possible to conclude that the second hypothesis fits better with the observed damage. Thus, it can be assured that the main cause for the bridge damage is related to a relative descend of the central piers. It is confirmed that the ground under the piers foundation is not stable enough. This circumstance might be caused by the river flow growth during the period of floods. As the bridge is located in an area where the river depicts a curve, the speed of water increases in the external area of the curve and

decreases in the internal one. Due to this effect, much sediment is accumulated around the lateral piers during the floods causing important erosions in the area of the central piers. The repeated effect of the floods could cause the foundation ground decrease; consequently its bearing capacity would decrease too, leading to relative descends downstream.

When such relative descends take place, the compression principal stress field concentrate converge to the most stiff pier support area. The deviation of the compression principal stress field leads to a tensile principal stress field normal to the axis of the bridge, in order to restore the standing balance. According to obtained results, such tensile stress field has become high enough to produce the longitudinal cracks observed in the arches.

## 5. CONCLUSIONS

In this paper a multidisciplinary approach to heritage documentation is presented involving Digital Photogrammetry, GPR and finite elements analysis. The surveying techniques have been proven to provide accurate information related to geometry, internal and external cracks, and current state of decay. It might be pointed out that since they are non contact demanding these fields can be analyzed avoiding decay aggravation. Another contribution might be highlighted. Information resulting from the photogrammetric process and the GPR test can be used to properly define a structural model which allows inferring the causes of the state of decay and further a prediction of the decay evolution can be derived too. For these all, it can be concluded that the described methodology can serve as a decision tool for the kind of reinforcing or restoration actions that might be accomplished to ensure the preservation of heritage masonry bridges.

## 6. REFERENCES

### References from Journals:

- Arias, P., Herráez, J., Lorenzo, H., Ordóñez, C., 2005. Control of structural problems in cultural heritage monuments using close-range photogrammetry and computer methods. *Computers & Structures*, 83, pp. 1754-1766.
- Benko, P., Martin, R. R., Varady, T., 2001. Algorithms for Reverse Engineering Boundary Representation Models. *Computer Aided Design*, 33 (11), pp. 839-851.
- Binda, L., Lenzi, G., Saisi, A., 1998. NDE of masonry structures: use of radar tests for the characterisation of stone masonries. *NDT&E International*, 31, pp. 411-419.
- Colla, C., Dast, P.C., McCann, D., Forde, M.C., 1997. Sonic, electromagnetic and impulse radar investigation of stone masonry bridges. *NDT&E International*, 30 (4), pp. 249-254.
- Flint, R.C., Jackson, P.D., McCann, D.M., 1999. Geophysical imaging inside masonry structures. *NDT&E International*, 32, pp. 469-479.
- Guidi, G., Beraldin, A., Atzeni, C., 2004. High-Accuracy 3-D Modeling of Cultural Heritage: The Digitizing of Donatello's "Maddalena". *IEEE Transactions on image processing*, 13 (3), pp. 370-380.

Jáuregui, D. V., White, K. R., Pate, J. W., Woodward, C. B., 2005. Documentation of Bridge Inspection Projects Using Virtual Reality Approach. *Journal of Infrastructures Systems*, 11 (3), pp. 172-179.

Lourenço, P., 2002. Computations on historic masonry structures. *Progress in Structural Engineering and Materials*, 4 (3), pp. 301-319.

Maierhofer, C., Leipold, S., 2001. Radar investigation of masonry structures. *NDT&E International*, 34, pp. 139-147.

Milani G., Lourenço, P.B, Tralli, A., 2006. Homogenised limit analysis of masonry wall, Part I: Failure surfaces. *Computers and Structures*, 84, pp. 166-180.

Pegon, P, Pinto, A.; Géradin, M., 2001. Numerical modelling of stone-block monumental structures. *Computers and Structures*, 79, pp. 2165-2181.

Ranalli, D., Scozzafava, M., Tallini, M., 2004. Ground penetrating radar investigations for the restoration of historic buildings: the case study of the Collemaggio Basilica (L'Aquila, Italy). *Journal of Cultural Heritage*, 5, pp. 91-99.

**References from Books:**

Bathe, K.J., 1996. *Finite Element Procedures*, Prentice Hall, New Jersey, USA.

Cooper M., Robson, S., 2001. Theory of Close Range Photogrammetry, In: Atkinson, K. B. *Close Range Photogrammetry And Machine Vision*, Whittles Publishing, Caithness, Scotland, UK, pp. 9-51.

**References from Other Literature:**

Alby, E., Grussenmeyer, P., Perrin, J. P., 2003. Integration of Close Range Photogrammetric Surveys in the Design Process of Architectural Projects. *Proceedings of CIPA XIX international Symposium*, Antalya, Turkey.

Clark, M., Forde, M., 2003. Using conductivity to determine the location of moisture in a masonry arch bridge. *Proceedings of the International Symposium (NDT-CE 2003)*.

Genovese R. A., 2005. Architectural, archaeologic and environmental restoration planning methodology: historic researches and techniques of survey aiming to conservation. *CIPA 2005 XX International Symposium*, Torino. Italy.

Toz, G., Duran, Z., 2004. Documentation and analysis of cultural heritage by photogrammetric methods and GIS: a case study. *Proceedings of ISPRS XX Congress*, Commission V, Istanbul, Turkey.